REPORT

NUCLEAR PHYSICS

Formation of α clusters in dilute neutron-rich matter

Junki Tanaka[1,2,3]*, Zaihong Yang[3,4]*, Stefan Typel[1,2], Satoshi Adachi[4], Shiwei Bai[5], Patrik van Beek[1], Didier Beaumel[6], Yuki Fujikawa[7], Jiaxing Han[5], Sebastian Heil[1], Siwei Huang[5], Azusa Inoue[4], Ying Jiang[5], Marco Knösel[1], Nobuyuki Kobayashi[4], Yuki Kubota[3], Wei Liu[5], Jianling Lou[5], Yukie Maeda[8], Yohei Matsuda[9], Kenjiro Miki[10], Shoken Nakamura[4], Kazuyuki Ogata[4,11], Valerii Panin[3], Heiko Scheit[1], Fabia Schindler[1], Philipp Schrock[12], Dmytro Symochko[1], Atsushi Tamii[4], Tomohiro Uesaka[3], Vadim Wagner[1], Kazuki Yoshida[13], Juzo Zenihiro[3,7], Thomas Aumann[1,2,14]

The surface of neutron-rich heavy nuclei, with a neutron skin created by excess neutrons, provides an important terrestrial model system to study dilute neutron-rich matter. By using quasi-free α cluster–knockout reactions, we obtained direct experimental evidence for the formation of α clusters at the surface of neutron-rich tin isotopes. The observed monotonous decrease of the reaction cross sections with increasing mass number, in excellent agreement with the theoretical prediction, implies a tight interplay between α-cluster formation and the neutron skin. This result, in turn, calls for a revision of the correlation between the neutron-skin thickness and the density dependence of the symmetry energy, which is essential for understanding neutron stars. Our result also provides a natural explanation for the origin of α particles in α decay.

Correlations and clustering are universal phenomena in composite systems for all scales of the material world, which range from the largest structures in the Universe to minute hadronic systems made of quarks. The atomic nucleus is a many-body quantum system that consists of nucleons, namely protons and neutrons. It can be described in the first approximation as nucleons moving independently in an attractive mean field generated by all nucleons. Their fermionic nature leads to the development of a shell structure with well-defined single-particle levels (*1*, *2*). This is the basis of the nuclear shell model that can take pairing and other residual interactions additionally into account (*1*–*3*). Correlations among nucleons play a decisive role in understanding the properties of atomic nuclei, nuclear matter, and giant objects in the Universe such as neutron stars (*4*). In nuclear matter, nucleons form light nuclear clusters that comprise deuterons (^{2}H), tritons (^{3}H), helions (^{3}He), and α particles (^{4}He) at densities sufficiently below the saturation density of nuclei (*5*). Deuteron-like clusters can also be found as short-range correlated pairs at higher densities (*6*–*8*). The α particle, as a compact four-nucleon correlation, plays a particular role because its strong binding is beneficial for the cluster formation.

Following the prediction of α-cluster formation (*9*, *10*) as reported in the 1930s for light self-conjugate nuclei (*11*), such as ^{8}Be, ^{12}C, and ^{16}O, microscopic theories on α clustering (*12*) have been developed that presume strong correlations between nucleons in clusters and weak intercluster correlations. In light nuclei, cluster structures are experimentally known to exist in their ground state as well as in excited states (*13*, *14*), specifically for states at energies in the vicinity of the cluster emission threshold (*15*). A prominent example is the Hoyle state (*16*) in ^{12}C with a three–α cluster structure at an excitation energy of 7.65 MeV (*17*). The existence of this state is crucial for the fusion of the three α clusters into a carbon nucleus in stars. This occurs at a rate that ensures a sufficient abundance of carbon, which is necessary for organic life, including human life (*18*).

Conversely, providing a consistent description of α clusters and nucleons on the same footing in heavy nuclei is challenging from a theoretical perspective (*19*). Although the formation of α clusters in heavy nuclei may be suggested from α decay according to the postulated model of Gamow (*19*, *20*), direct experimental evidence has not yet been reported. Theoretical studies have suggested that, similar to dilute nuclear matter, there exists a certain probability that α clusters can form in the ground state of heavy nuclei at the very surface of the nucleus—that is, the region outside the saturated nuclear core—with densities below the α-cluster dissolution threshold (the Mott density) (*5*, *21*, *22*). This feature could potentially explain the origin of α particles in the α-decay process. This surface α-clustering phenomenon also occurs in neutron-rich heavy nuclei that feature a neutron skin created by the excess neutrons and are generally stable against α decay (*4*, *23*). In this case, however, there is a close interplay between this surface α-clustering effect and the neutron-skin thickness, as suggested by recent generalized relativistic density functional (gRDF) calculations (*5*, *23*). This model predicts a reduction of the neutron-skin thickness in comparison to theoretical calculations without considering the α-clustering effect, which will further affect our understanding of the nuclear equation of state (*5*, *23*). As a result of this interplay, the formation of α clusters also gets hindered by the development of a neutron skin in heavy nuclei. The tin isotopic chain with a proton magic number $Z = 50$ provides an ideal testing ground to study this intriguing interplay. The bulk and surface properties of these nuclei are not strongly dependent on the details of the nuclear structure and can be well described by relativistic mean-field theories (*23*) [see fig. S1 and table S5 for the comparison between theoretical calculated radii (*23*) and the experimental data]. According to the gRDF calculation, the probability of α-cluster formation gradually decreases along the tin isotopic chain when progressing from the stable ^{112}Sn to the very neutron-rich ^{132}Sn, which is accompanied by a steady increase in the neutron-skin thickness (*23*). Therefore, we performed an experiment with tin isotopes to examine the probability of finding α clusters [hereafter defined as "the effective number of α clusters (*23*)"] in stable heavy nuclei and to study its isotopic dependence. Our experiment covers stable nuclides from ^{112}Sn to ^{124}Sn (see table S2 for detailed properties of the target materials), with neutron numbers from N = 62 to 74.

The most direct access to α clustering in the ground state of nuclei is the proton-induced α-knockout reaction (p, $p\alpha$). Quasi-free knockout reactions of the type (e, ep) and (p, pp) are well-established methods to investigate the single-particle structures of nuclei (*24*); quasi-free (p, $p\alpha$) reactions were also used extensively in the 1970s and 1980s to study α clustering in light- and medium-mass stable nuclei (*25*–*27*). By measuring the momenta and angles of the light particles involved in the scattering

[1]Technische Universität Darmstadt, Fachbereich Physik, Institut für Kernphysik, Schlossgartenstraße 9, 64289 Darmstadt, Germany. [2]GSI Helmholtz Center for Heavy Ion Research GmbH, Planckstraße 1, 64291 Darmstadt, Germany. [3]RIKEN Nishina Center for Accelerator-Based Science, 2-1 Hirosawa, Wako 351-0198, Japan. [4]Research Center for Nuclear Physics, Osaka University, 10-1 Mihogaoka, Ibaraki 567-0047, Japan. [5]State Key Laboratory of Nuclear Physics and Technology, School of Physics, Peking University, Beijing 100871, China. [6]Université Paris-Saclay, CNRS/IN2P3, IJCLab, 91405 Orsay, France. [7]Department of Physics, Kyoto University, Kitashirakawa-Oiwake, Sakyo, Kyoto 606-8502, Japan. [8]Faculty of Engineering, University of Miyazaki, 1-1 Gakuen, Kibanadai-nishi, Miyazaki 889-2192, Japan. [9]Cyclotron and Radioisotope Center, Tohoku University, 6-3 Aoba, Aramaki, Aoba-ku, Sendai 980-8578, Japan. [10]Department of Physics, Tohoku University, Sendai 980-8578, Japan. [11]Department of Physics, Osaka City University, Osaka 558-8585, Japan. [12]Center for Nuclear Study, The University of Tokyo, 2-1 Hirosawa, Wako 351-0198, Japan. [13]Advanced Science Research Center, Japan Atomic Energy Agency, Tokai, Ibaraki 319-1195, Japan. [14]Helmholtz Research Academy Hesse for FAIR, Schlossgartenstraße 9, 64289 Darmstadt, Germany.
***Corresponding author. Email: zhyang@ribf.riken.jp (Z.Y.); junki.tanaka@riken.jp (J.T.)**

process, the intrinsic momentum of the knocked-out particle and its binding energy in the nucleus can be reconstructed from the conservation of energy and momentum. For the (p, $p\alpha$) experiment reported herein, the experimental setup was designed according to the quasi-free scattering kinematics of protons on α particles bound in tin isotopes. For this investigation, we selected a large center-of-mass scattering angle, i.e., a large momentum is transferred to the α particle at the instance of the reaction and the residue can be regarded safely as a spectator (see fig. S2). Therefore, the observed α particles in the final state, detected in coincidence with the scattered protons, directly reflect the probability of finding α clusters in the target nucleus. By measuring the (p, $p\alpha$) cross sections under quasi-free kinematic conditions, the change in the effective number of α clusters in the tin isotopic chain can be obtained as a function of the neutron number.

The experiment was performed at the nuclear experimental facility in the Research Center for Nuclear Physics (RCNP), Osaka University. Figure 1 shows the experimental setup. A 392-MeV proton beam with an intensity of 100 nA, provided by a ring cyclotron, impinged on a tin target. Information on the targets and beam intensities is specified in Table 1. After the (p, $p\alpha$) reaction, the scattered protons were analyzed by using the Grand Raiden magnetic spectrometer (*28*). It was set at 45.3° with respect to the proton beam, and the energies and momenta were deduced from the position and angles measured at the focal plane. The coincident α particles were detected at 60° by the large acceptance spectrometer (LAS) (*29*). The acceptance was mainly determined by using a slit with a well-defined rectangular aperture at the entrance of the Grand Raiden spectrometer. Each type of particle was identified in the corresponding focal-plane detectors for the Grand Raiden and LAS instruments, as shown in Fig. 1.

Figure 2A presents the coincident timing spectrum of the recorded proton-α pair in the time window of the 500-ns coincidence gate. It includes seven peaks separated by time intervals of 62.5 ns, which correspond to the time structure of the beam bunches from the cyclotron. Although accidental-coincidence events are dominant, an enhancement in the third bunch, which arises from true-coincidence events, is observed. From the measured kinetic energies of the protons, T_p, and α particles, T_α, in the coincident bunch, the missing-mass spectrum, M_X = 392 MeV − T_p − T_α, is constructed (black points in Fig. 2B). The blue points in Fig. 2B correspond to the background spectrum resulting from the accidental-coincidence bunches after proper normalization. The spectrum from the true-coincidence bunch shows a prominent peak on top of the background.

We subtracted the "accidental-coincidence" background from the "true-coincidence" spectrum. The error bars presented in Fig. 3, A to D, include the effect of this subtraction. The missing-mass spectra for the targets—^{112}Sn, ^{116}Sn, ^{120}Sn, and ^{124}Sn—were obtained with a resolution of 0.83(3) MeV (standard deviation) and fitted using the Gaussians for the ground-state peaks and the simulated shapes of the continuum (fitting parameters in table S3). The peak positions of the ground state for the different targets agree well with the known α-separation energies. This result clearly indicates the preformation of α particles in these tin isotopes. The observed momentum distribution of the α particles (fig. S3) is also in good agreement with the theoretical prediction (*23*), reaffirming that the formation of α particles indeed occurs in the low-density surface region of heavy nuclei as predicted by the gRDF calculation (*23*).

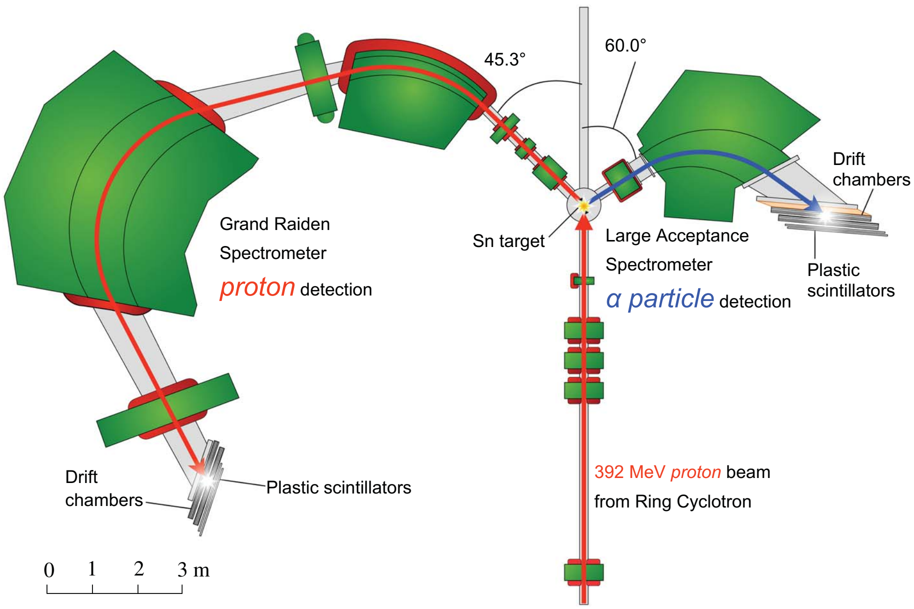

Fig. 1. Schematic illustration of the experimental setup. A 392-MeV proton beam from the ring cyclotron accelerator impinges on a tin target. After a ^{A}Sn(p, $p\alpha$)$^{A-4}$Cd reaction, a scattered proton is detected by the focal-plane detectors, drift chambers, and plastic scintillators after traversing the Grand Raiden spectrometer at an angle of 45.3° with respect to the proton beam. A knocked-out α particle is detected by the focal-plane detectors behind the LAS spectrometer at an angle of 60.0° with respect to the proton beam.

Table 1. Experimental and theoretical values of the tin isotope parameters. Target thicknesses and enrichments of the tin-isotope targets, the experimental and theoretical cross sections, the effective number of α clusters, and the theoretical neutron-skin thicknesses Δr_{np} from the gRDF prediction (*23*). The calculations were performed with the DD2 parameters (*5*) for the effective interaction without and with the α clusters. In the last column, the value is the percentage by which Δr_{np} is reduced when α clusters are included. nb, nanobarn.

Tin isotope	Target thickness (mg/cm^2)	Isotopic enrichment (%)	Experimental cross sections (nb)	Theoretical cross sections (nb)	Effective number of α clusters	Theoretical Δr_{np} without α (fm)	Theoretical Δr_{np} with α (fm)	Relative Δr_{np} change (%)
^{112}Sn	40.2(4)	95.1(1)	0.157(12)	0.160	0.3876	0.0495	0.0277	−44
^{116}Sn	39.3(4)	97.8(2)	0.129(16)	0.127	0.3304	0.0843	0.0580	−31
^{120}Sn	39.9(4)	99.6(1)	0.090(13)	0.095	0.2668	0.1179	0.0912	−23
^{124}Sn	40.7(4)	97.4(2)	0.073(10)	0.065	0.1958	0.1505	0.1275	−15

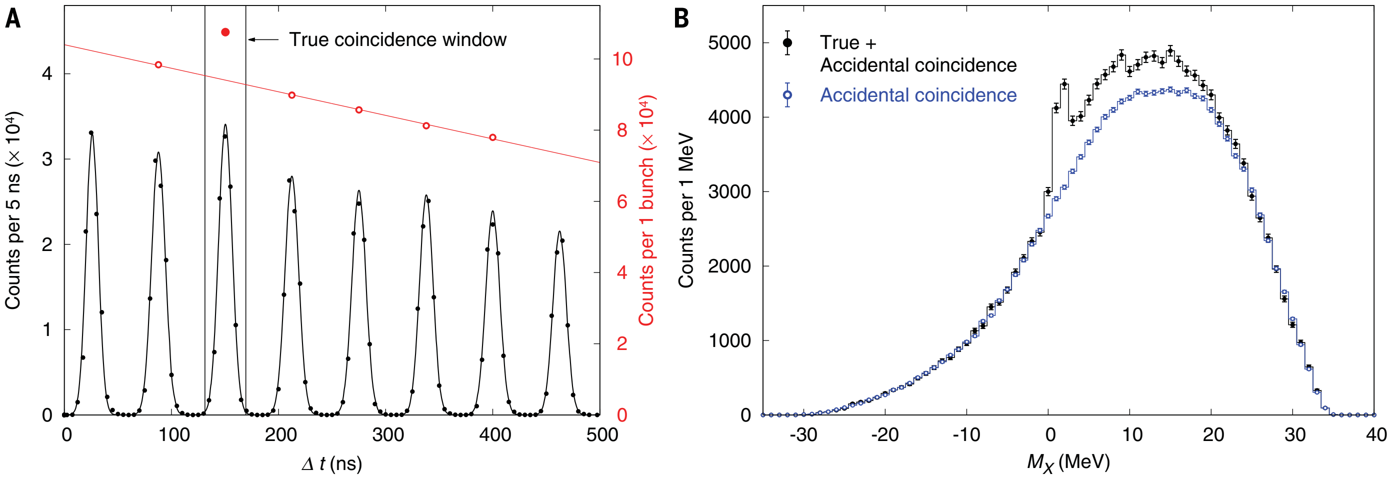

Fig. 2. Accidental-coincidence background distributions from the coincident timing spectrum and missing-mass spectrum for the ^{112}Sn target. (**A**) Coincident time spectrum of the protons and α particles in the time window of the 500-ns coincidence gate. (**B**) Missing-mass spectrum (black: true and accidental-coincidence events; blue: only accidental-coincidence events. The error bars are statistical only. In (B), the amplitude of the accidental-coincidence background within the true-coincidence time window is determined from the linear fitting [the red line in (A)] of the statistics of the accidental-coincidence peaks. Similar plots for the other three tin isotope targets are presented in fig. S5.

To study the isotopic dependence of the α-formation probability, we then deduced the cross sections from the reaction yields by integrating the ground-state peaks (the black dashed-dotted line in Fig. 3, A to D), which are given in Table 1. Note that the instrumental ("accidental-coincidence") background has already been removed as discussed above. Figure 3E displays the results of the isotopic dependence of the (p, $p\alpha$) cross sections. The associated errors are dominated by the statistical errors but also include the systematical errors (~1.6%). (Details are given in the methods.) We observe a gradual decrease in the cross section with increasing mass numbers. The cross section for ^{112}Sn is larger by a factor of 2.2(3) as compared to that for ^{124}Sn. This is in line with the predicted isotopic dependence of the effective numbers of the α clusters (Table 1 and Fig. 3F). The radial density distributions of the α clusters in the gRDF approach were incorporated into a distorted-wave reaction model in the impulse approximation with a proton optical potential (*30*) and an elastic proton-α cross section (*31*) (see methods). These were used to obtain the theoretical (p, $p\alpha$) cross sections while considering the experimental conditions of the angular and momentum acceptances. Although the α particles were emitted in the direction opposite to the core nuclei after the reactions under the selected kinematic condition in the experiment, the absorption of the α particles was considered by introducing a proper optical potential (*32*, *33*). The imaginary potential depth was rescaled to obtain theoretical cross sections that almost match with the experimental ones, but the scaling factor was kept identical for all Sn nuclei. The points of origin of the α particles were sampled according to the probability of finding them on the surface of the target nuclei in the gRDF calculation (*23*). The scaling factor of 0.148 for the imaginary potential depth is rather small. This indicates that the α particle is hardly absorbed by the residual nucleus after being hit by the incident proton. The dependence of the (p, $p\alpha$) reaction cross section on the mass number A of the target nucleus is depicted in Fig. 3E. The isotopic trend of the theoretical cross sections is very robust against variations in the optical potential radius R and the diffuseness parameter a. This was explored in trial calculations by varying R and a by about 15%, which covers the typical range of these quantities. The theoretical isotopic dependence closely follows the experimentally determined one; in fig. S6, the linear relationship between the theoretical cross sections and the experimental cross sections is clearly observed [Pearson's correlation coefficient (r) = 0.9934, P = 0.0066]. We emphasize that the reduction of the cross section by a factor of about two when going from ^{112}Sn to ^{124}Sn cannot be attributed to the systematic change of the proton optical potential (*32*) with the mass number or that of the α-particle optical potential (*33*), because the volume integrals of the imaginary part vary by only 15.3 and 8.9%, respectively. This is reaffirmed by the experimental and theoretical σ/N_α ratios of all the isotopes used in the experiment, given in Fig. 3G, where σ is the experimental cross section and N_α is the number of α particles. An almost flat distribution is obtained for σ/N_α, demonstrating that the decline in the measured cross sections with an increasing mass number is indeed predominantly caused by the decrease in N_α. Note that the decrease of σ and N_α is also correlated with the increase of the α-particle binding energy with the mass number A. Because the α-particle density distribution, in particular the shape and position, and the binding energy are determined self-consistently in the gRDF calculations, only a change of the parametrization of the interaction can help to lift this correlation, which is beyond the scope of the present work. However, the change of the α-particle density distribution and the α-particle binding energy should have a minor contribution to the reduction of the cross section, as is evident from the almost constant σ/N_α ratio. Hence, the observed reduction of the cross section with increasing mass number reflects the decrease of the effective number of α particles N_α, depicted in Fig. 3F.

The neutron-skin thickness $\Delta r_{\rm np}$ is defined as the difference between the root-mean-square radius of the neutron density distribution $r_{\rm n}$ and that of the proton density distribution $r_{\rm p}$, $\Delta r_{\rm np} = r_{\rm n} - r_{\rm p}$. For heavy nuclei, it is closely related to the density dependence of the symmetry energy in the nuclear equation of state (EOS) (*34*). The correlation between $\Delta r_{\rm np}$ and the slope parameter L (neutron-matter pressure) in the EOS (*35*) is a linear function when the results of many mean-field model calculations are compiled (*36*). Therefore, L can be deduced from $\Delta r_{\rm np}$. According to the gRDF framework, the existence of α clusters on the nuclear surface will reduce the size of the neutron skin (*23*). The theoretical $\Delta r_{\rm np}$ for the tin isotopes used in this experiment with and without considering the α-cluster effect are given in Table 1, which indicates a reduction of 15 to 44%. This effect necessitates a correction to the relationship between

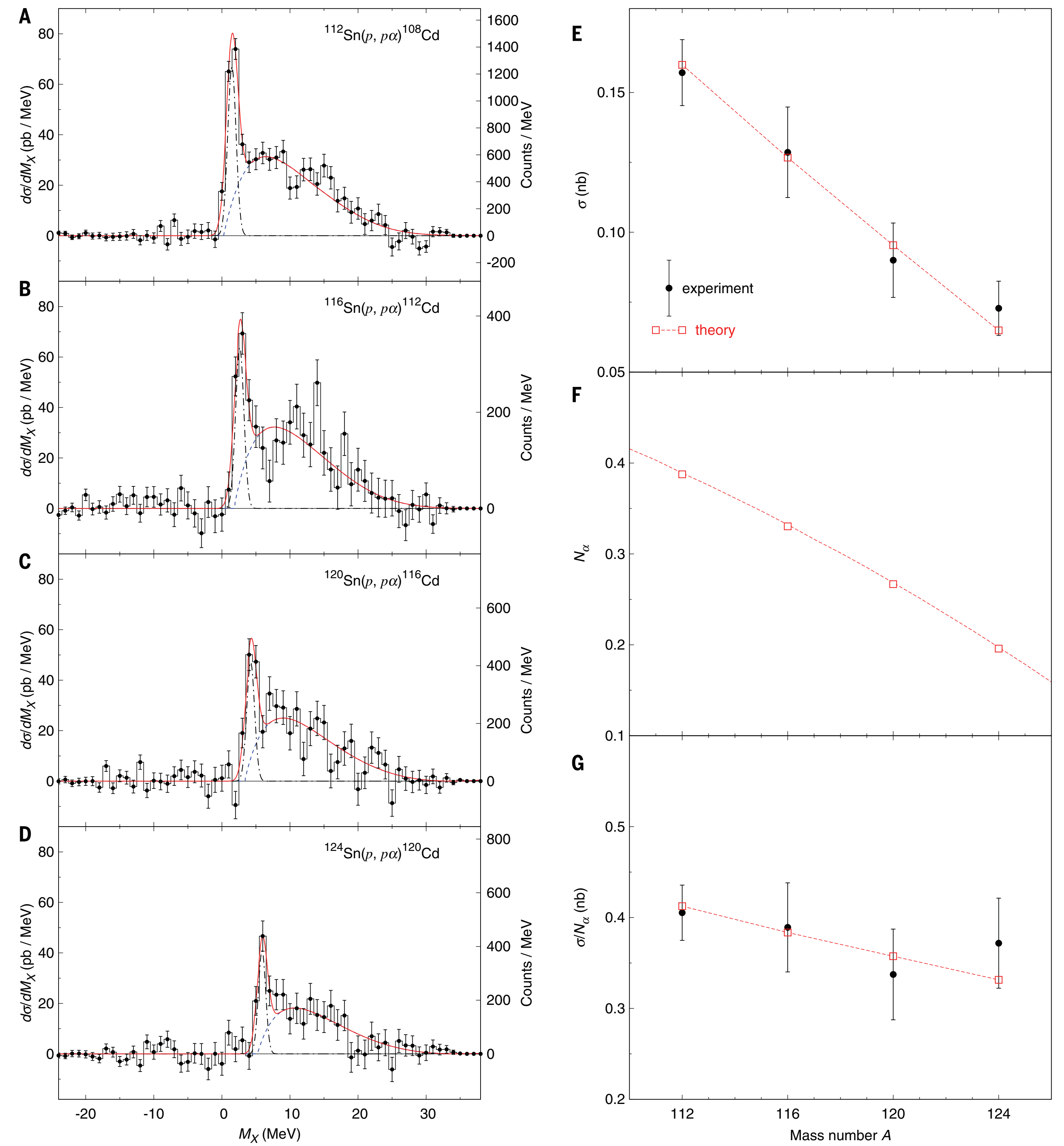

Fig. 3. Missing-mass spectra for the α-knockout reactions, the isotopic dependence of the (*p*, *p*α) cross sections, and a comparison with the theoretical calculations. (**A** to **D**) Missing-mass spectra for the α-knockout reactions for tin targets (A) ^{112}Sn, (B) ^{116}Sn, (C) ^{120}Sn, and (D) ^{124}Sn. The effect of a small dip between the ground state peak and the broad continuous bump in (B) on the count of the peak is within the fitting error and does not change the conclusions of this study. The red lines in (A) to (D) represent the results of the fits with the Gaussians for the ground-state peaks (the black dashed-dotted lines) and the simulated shapes of the continuum (the blue dashed lines). They include the experimental acceptances of the momenta and the geometric cuts. (**E**) Isotopic dependence of the cross sections, as determined experimentally (black points) and theoretically (red line). (**F**) Dependence of the effective number of α clusters, N_α, on the mass number *A* of the tin nuclei in the calculation using the gRDF approach (*23*) with the DD2 parameters (*5*). (**G**) Ratios of the cross sections σ and N_α. In (A) to (D), the error bars are statistical only; in (E) and (G), the error bars are dominated by the statistical errors but also include the systematical errors (~1.6%). (Details are given in the methods.) In (E) and (G), the correlated normalization uncertainty of the theoretical values is not presented because it is canceled out when we discuss the isotopic dependence of σ and σ/N_α.

Δr_{np} and L (*35*) that goes beyond the mean-field calculations without considering the formation of α clusters. Knowledge of the EOS for neutron-rich matter is of fundamental importance in nuclear physics and for understanding the properties of neutron stars (*4*). The result reported herein supports the close correlation between the surface α clustering and the neutron-skin thickness in heavy nuclei as predicted by the gRDF calculations (*23*). The Δr_{np} of tin isotopes can be better reproduced by relativistic mean-field calculations after considering the α-clustering effect. (A comparison between the experimental data and the theoretical calculations can be found in fig. S4.) The existence of α clusters on the nuclear surface needs to be considered for determining L from Δr_{np}. It is worthwhile to mention that short-range correlated pairs in neutron-rich nuclei (*6*, *7*) may have similar effects in reducing the neutron-skin thickness (*37*). Recent ab initio many-body calculations of ^{48}Ca also show the necessity to refine nuclear density functionals and to reassess the correlation of the neutron skin thickness with isovector properties of the nuclear EOS (*38*). We expect that such ab initio calculations will be extended to even heavier nuclei and will explicitly take into account the effect of nuclear clustering in the future.

We have measured the cross sections for the proton-induced quasi-free α-cluster knockout reactions along the tin isotopic chain, ^{A}Sn$(p, p\alpha)^{A-4}$Cd. Our results provide direct evidence for the formation of α clusters in the dilute neutron-rich matter such as the surface of neutron-rich heavy nuclei. The measured cross sections along the isotopic chain decrease smoothly, but substantially, with the neutron number. The theoretical analysis attributes this decrease to the interplay between α-cluster formation and the neutron skin, which further affects our understanding of the nuclear EOS (*4*, *5*, *23*). Extensive efforts across the world are ongoing to measure the neutron-skin thicknesses of nuclei with sufficient precision (*35*). In particular, parity-violating electron scattering experiments at Jefferson Lab are expected to provide more accurate measurements of the neutron-skin thickness of ^{208}Pb and ^{48}Ca (*39*, *40*). To accurately constrain the nuclear EOS, our result also suggests the necessity of considering the effect of nuclear clustering when deducing constraints for the EOS parameters from the observed parity-violating asymmetry and neutron-skin thickness. The formation of α-clusters at the surface of heavy nuclei can be a natural explanation for the "α-particle preformation factor" that is postulated in the theory of α decay (*19*, *20*). Future experiments with radioactive α emitters, which are produced as high-energy secondary beams with radioactive-beam facilities such as the Radioactive Isotope Beam Factory (RIBF), GSI Helmholtzzentrum für Schwerionenforschung GmbH (GSI), and Facility for Antiproton and Ion Research (FAIR) could elucidate this relationship.

REFERENCES AND NOTES

1. P. Ring, P. Schuck, *The Nuclear Many-Body Problem* (Springer, 1980).
2. T. Otsuka, A. Gade, O. Sorlin, T. Suzuki, Y. Utsuno, *Rev. Mod. Phys.* **92**, 015002 (2020).
3. D. J. Dean, M. Hjorth-Jensen, *Rev. Mod. Phys.* **75**, 607–656 (2003).
4. M. Oertel, M. Hempel, T. Klähn, S. Typel, *Rev. Mod. Phys.* **89**, 015007 (2017).
5. S. Typel, G. Röpke, T. Klähn, D. Blaschke, H. H. Wolter, *Phys. Rev. C* **81**, 015803 (2010).
6. O. Hen, G. A. Miller, E. Piasetzky, L. B. Weinstein, *Rev. Mod. Phys.* **89**, 045002 (2017).
7. O. Hen *et al*., *Science* **346**, 614–617 (2014).
8. R. Subedi *et al*., *Science* **320**, 1476–1478 (2008).
9. H. A. Bethe, R. F. Bacher, *Rev. Mod. Phys.* **8**, 82–229 (1936).
10. W. Wefelmeier, *Z. Phys.* **107**, 332–346 (1937).
11. H. Morinaga, *Phys. Rev.* **101**, 254–258 (1956).
12. H. Margenau, *Phys. Rev.* **59**, 37–47 (1941).
13. J. P. Ebran, E. Khan, T. Nikšić, D. Vretenar, *Nature* **487**, 341–344 (2012).
14. M. Freer, H. Horiuchi, Y. Kanada-En'yo, D. Lee, U.-G. Meißner, *Rev. Mod. Phys.* **90**, 035004 (2018).
15. K. Ikeda, N. Takigawa, H. Horiuchi, *Prog. Theor. Phys. Suppl.* **E68**, 464–475 (1968).
16. F. Hoyle, *Astrophys. J. Suppl. Ser.* **1**, 121 (1954).
17. C. W. Cook, W. A. Fowler, C. C. Lauritsen, T. Lauritsen, *Phys. Rev.* **107**, 508–515 (1957).
18. H. O. U. Fynbo *et al*., *Nature* **433**, 136–139 (2005).
19. C. Qi, R. J. Liotta, R. A. Wyss, *Prog. Part. Nucl. Phys.* **105**, 214–251 (2018).
20. G. Gamow, *Z. Phys.* **51**, 204–212 (1928).
21. D. S. Delion, R. J. Liotta, *Phys. Rev. C* **87**, 041302(R) (2007).
22. K. Hagel *et al*., *Phys. Rev. Lett.* **108**, 062702 (2012).
23. S. Typel, *Phys. Rev. C* **89**, 064321 (2014).
24. G. Jacob, Th. A. J. Maris, *Rev. Mod. Phys.* **38**, 121–142 (1966).
25. T. A. Carey, P. G. Roos, N. S. Chant, A. Nadasen, H. L. Chen, *Phys. Rev. C* **23**, 576–579 (1981).
26. N. S. Chant, P. G. Roos, *Phys. Rev. C* **15**, 57–68 (1977).
27. P. G. Roos *et al*., *Phys. Rev. C* **15**, 69–83 (1977).
28. M. Fujiwara *et al*., *Nucl. Instrum. Meth. A* **422**, 484–488 (1999).
29. T. Wakasa, K. Ogata, T. Noro, *Prog. Part. Nucl. Phys.* **96**, 32–87 (2017).
30. M. Toyokawa, K. Minomo, M. Yahiro, *Phys. Rev. C* **88**, 054602 (2013).
31. K. Yoshida, K. Minomo, K. Ogata, *Phys. Rev. C* **94**, 044604 (2016).
32. S. Hama, B. C. Clark, E. D. Cooper, H. S. Sherif, R. L. Mercer, *Phys. Rev. C* **41**, 2737–2755 (1990).
33. M. Nolte, H. Machner, J. Bojowald, *Phys. Rev. C* **36**, 1312–1316 (1987).
34. B. A. Brown, *Phys. Rev. Lett.* **85**, 5296–5299 (2000).
35. X. Roca-Maza, N. Paar, *Prog. Part. Nucl. Phys.* **101**, 96–176 (2018).
36. X. Roca-Maza, M. Centelles, X. Viñas, M. Warda, *Phys. Rev. Lett.* **106**, 252501 (2011).
37. G. A. Miller *et al*., *Phys. Lett. B* **793**, 360–364 (2019).
38. G. Hagen *et al*., *Nat. Phys.* **12**, 186–190 (2016).
39. S. Abrahamyan *et al*., *Phys. Rev. Lett.* **108**, 112502 (2012).
40. C. J. Horowitz, K. S. Kumar, R. Michaels, *Eur. Phys. J. A* **50**, 48 (2014).
41. J. Tanaka *et al*., Numerical data for "Formation of α clusters in dilute neutron-rich matter." Zenodo (2020); https://doi.org/10.5281/zenodo.4290691.

ACKNOWLEDGMENTS

We thank RCNP staff for their hospitality and acknowledge experimental support from RCNP ring cyclotron operational staff and Grand Raiden supporting scientific staff. We thank the local technical staff at the RCNP for aid during the preparation of the experiment. We thank the GSI target laboratory for the preparation of the targets. **Funding:** This work was partially supported by the Deutsche Forschungsgemeinschaft (DFG, German Research Foundation) Project-ID 279384907 - SFB 1245, by the GSI-TU Darmstadt cooperation agreement, by the BMBF (project 05P19RDFN1), and in part by Grants-in-Aid of the Japan Society for the Promotion of Science (grant no. JP16K05352). Z.Y. acknowledges support from the Foreign Postdoctoral Researcher program of RIKEN. **Author contributions:** T.A., S.T., T.U., and Z.Y. proposed the experiment. Z.Y. and J.Z. designed the experimental setup and led the test experiments. Z.Y. and J.T. conducted the necessary experimental preparations and also executed the experiment. J.T. and Z.Y. performed the data reduction and analysis presented here. J.T., S.T., T.A., and Z.Y. prepared the draft of the manuscript. All authors read the manuscript, gave comments, suggested changes, and agreed with the final version. S.T. provided the original theoretical idea and performed the reaction calculations with contributions from K.O. and K.Y. A.T. and N.K., along with the Grand Raiden and LAS support team, took responsibility for the operation of the spectrometers. Y.Mat. and A.T. upgraded the drift chambers of the LAS spectrometer with the help of staff at RIKEN, RCNP, and Konan University. D.S., S.A., V.P., V.W., Y.K., W.L., S.Hu., Y.J., and J.L. prepared the experimental setup with the local group. P.v.B., Y.F., S.He., A.I., Y.J., M.K., N.K., J.H., S.B., K.M., Y.Mae., S.N., H.S., F.S., and P.S. supervised the experiment and verified that the data were acquired correctly. **Competing interests:** The authors declare that they have no competing financial interests. **Data and materials availability:** The data that support the findings of this study have been presented in the main text and supplementary materials. The data underlying the figures are accessible at Zenodo (*41*).

SUPPLEMENTARY MATERIALS

science.sciencemag.org/content/371/6526/260/suppl/DC1
Materials and Methods
Figs. S1 to S6
Tables S1 to S5
References (*42*–*47*)

24 August 2020; accepted 30 November 2020
10.1126/science.abe4688

Science

Formation of # clusters in dilute neutron-rich matter

Junki TanakaZaihong YangStefan TypelSatoshi AdachiShiwei BaiPatrik van BeekDidier BeaumelYuki FujikawaJiaxing HanSebastian HeilSiwei HuangAzusa InoueYing JiangMarco KnöselNobuyuki KobayashiYuki KubotaWei LiuJianling LouYukie MaedaYohei MatsudaKenjiro MikiShoken NakamuraKazuyuki OgataValerii PaninHeiko ScheitFabia SchindlerPhilipp SchrockDmytro SymochkoAtsushi TamiiTomohiro UesakaVadim WagnerKazuki YoshidaJuzo ZenihiroThomas Aumann

Science, 371 (6526), • DOI: 10.1126/science.abe4688

 # particles in stable nuclei
Decay is a common mode of radioactivity in heavy elements such as uranium that entails the loss of particles comprising two protons and two neutrons. Despite more than a century of study, when and where these # particles form in stable and unstable nuclei alike remains an open question. Tanaka *et al.* bombarded a series of stable tin isotopes with high-energy protons and detected ejected # particles at an abundance inversely correlated with mass number (see the Perspective by Hen). This observation, relating # particle accumulation to the neutron skin thickness at the nuclear surface, bears on models spanning radioactive decay to neutron star dynamics.

Science, this issue p. 260; see also p. 232

Science (ISSN 1095-9203) is published by the American Association for the Advancement of Science. 1200 New York Avenue NW, Washington, DC 20005. The title *Science* is a registered trademark of AAAS.